

Scanning Shack-Hartmann sensor for wavefront measurements on freeform optics

Martin Fuerst, Nikolaus Berlakovich, Ernst Csencsics, and Georg Schitter

Automation and Control Institute (ACIN), TU Wien, Gusshausstrasse 27-29, Vienna, Austria

ABSTRACT

The Shack-Hartmann wavefront sensor has the potential to directly characterize the optical performance of a freeform part by measuring the wavefront transmitted or reflected by the part. However, the traditional Shack-Hartmann sensor's small dynamic range and aperture limit its applicability on strongly curved or extended freeform parts. The combination of a Shack-Hartmann sensor with a highly precise positioning system and a suitable registration algorithm can overcome these limitations. This paper presents an integrated and fully automated measurement system that is based on a scanning Shack-Hartmann sensor, demonstrates the enabled dynamic range extension, and presents measurement results obtained from a microscope objective with a numerical aperture of 0.65. The results show the capability of measuring a wavefront with an opening angle of $\pm 80^\circ$ and detecting an rms wavefront error of 0.28λ .

Keywords: Optical metrology, wavefront sensing, mechatronics, Shack-Hartmann sensor

1. INTRODUCTION

Freeform and metaform optics are expected to be one of the driving forces of innovation in the optical industry of the next decades.¹ Freeform optics have already been shown to be capable of enhancing an optical systems' performance by reducing its weight, size, number of elements and optical aberrations.² The main drawback of aspherical and freeform optical components is that they are much more difficult to manufacture and to align than spherical components.³ Especially in an industrial environment, such as during production, the quality of freeform parts is more challenging to monitor than the quality of classical, spherical optics. However, there is a mutual characteristic in the metrology of classical and modern optical parts:⁴ The qualification typically relies on *shape* measurements of the optical component, which are either collected by areal, interferometric methods or single-point-probe based profilometry methods.⁵

These shape measurements are most often performed with either interferometric techniques or stylus-based approaches. Interferometric methods offer high precision and sub-nm resolution and are thus commonly used for testing optical elements with low numerical aperture (NA).^{5,6} For highly divergent (e.g. high-NA focusing optics) or freeform wavefronts, however, null-elements are required, which can be realized through a "golden master" reference optic or computer generated holograms (CGHs).⁷ The drawback of both approaches is a reduced versatility of the measurement tool and an additional source of uncertainty in the measurement process. The profilometric or coordinate-based methods are very versatile and can be equipped with tactile or non-tactile probes, and offer resolutions comparable to the interferometric approach.^{5,8} To avoid damaging delicate coating, optical parts are typically measured with non-tactile probes.⁹ The main drawback of CMMs and profilometers is that they are typically much slower, as the surface data has to be acquired point-by-point or line-by-line.

To avoid the drawbacks of shape measurements altogether, it was proposed to directly measure the part's *optical performance*.⁴ This may be achieved by measuring the shape of the optical wavefront that is transmitted or reflected by an optical part or system. The Shack-Hartmann sensor (SHS) is a camera-based sensor that measures the shape of an incoming wavefront region in a single shot and is small, robust, fast and comparatively insensitive to vibrations, making it well suited for industrial environments.^{10,11} The SHS's capability to characterize lenses

Further author information: (Send correspondence to M. Fuerst or N. Berlakovich)

M. Fuerst: E-mail: fuerst2@acin.tuwien.ac.at, Telephone: +43 (0)1 588 01 - 376 514

N. Berlakovich: E-mail: berlakovich@acin.tuwien.ac.at, Telephone: +43 (0)1 588 01 - 376 529

bigger than the sensor aperture by manual, linear repositioning of the sensor and subsequent stitching of the acquired wavefront subaperture images, was recently demonstrated.^{12,13} However, the SHS is limited when it comes to the measurement of highly divergent wavefronts.¹⁴

Recently, an approach was published that bypasses the limitations of the Shack-Hartmann sensor by mechanically repositioning the sensor along the wavefront.¹⁵ The idea is to increase the measurement distance and thereby reduce the curvature of the incident wavefront on the sensor. In this case, only a part of the entire wavefront is observed in a single wavefront image, such that the sensor needs to be moved to multiple positions along the wavefront for collecting a number of partial images (or “subapertures”). The collected data is then interpreted in combination with the positioning data to obtain the complete wavefront. However, the presented setup is only partially automated, as the sensor positions and orientations are pre-planned based on the expected wavefront shape, limiting its applicability for arbitrary optics.¹⁵ To overcome this limitation, a strategy for automatic tangential alignment is developed¹⁶ and performance limits concerning the positioning uncertainties in relation to the desired wavefront sensitivity are discussed.¹⁷ The feasibility of the approach is shown with a 3-degree-of-freedom (DoF) positioning device enabling circular trajectories and single-axis rotations.

The contribution of this paper is the extension of the principle to a 5 degree-of-freedom positioning system and the experimental validation of the system’s capability to directly measure a highly divergent wavefront, such as generated by a microscope objective or, in extension, a focusing freeform optical part or system.

Section 2 describes how the limited dynamic range of the Shack-Hartmann sensor can be overcome through feedback-controlled repositioning and Section 3 introduces the experimental setup designed to test the approach and the required registration algorithms. Finally, Section 4 presents measurement results acquired on a high-NA microscope objective and Section 5 concludes the paper and gives an outlook on proposed future work.

2. SCANNING SHACK-HARTMANN SENSOR

The Shack-Hartmann sensor is based on sampling an incident wavefront via a lenslet array onto an image sensor.¹⁰ This means, that for a perfect plane wavefront, an evenly spaced spot pattern is registered, while local wavefront gradients lead to spot displacements. From the registered displacements, the local gradients can be calculated and the incident wavefront shape can be reconstructed. This principle is illustrated in Figure 1a). The crucial technical parameters of an SHS are its lenslet number, its lenslet pitch and its focal length. The same parameters lead to its fundamental performance limits, illustrated in Figure 1b) and c). High incident slopes or large curvatures lead to ambiguities in the assignment of detected spots to their reference positions. For typically available Shack-Hartmann sensors, these limits are given as $1 - 5^\circ$ for global tilt and minimum radius of curvature of $r_{min} \approx 3 \cdot f_L$.¹⁷ With advanced spot assignment algorithms, the range can be extended to about $10 - 15^\circ$,¹⁸ which is however still insufficient for the large opening angle of high-NA or freeform optics.

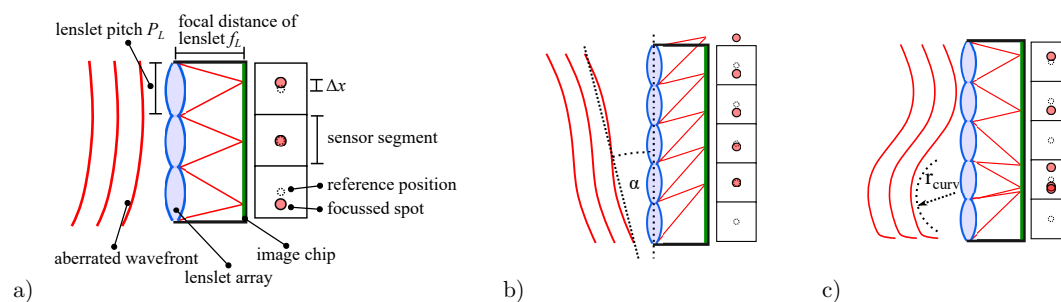


Figure 1. Dynamic range limitations of the SHS. a) SHS working principle based on detection of a spot pattern generated by focussing lenslets. b) Maximum wavefront tilt α , determined by the ratio of lenslet focal length and lenslet diameter. c) Maximum admissible wavefront curvature r_{curv} causing multiple spots to fall into the same sensor segment (adapted from Ref. 17).

To avoid these limits, the approach illustrated in Figure 2 is proposed. By increasing the measurement distance of the SHS, the curvature can be reduced, while realignment keeps the absolute tilt low. The downside is that only a portion of the wavefront is recorded in this way, meaning that for a global representation of the wavefront, multiple subapertures need to be recorded which need to be combined by suitable stitching or registration algorithms.

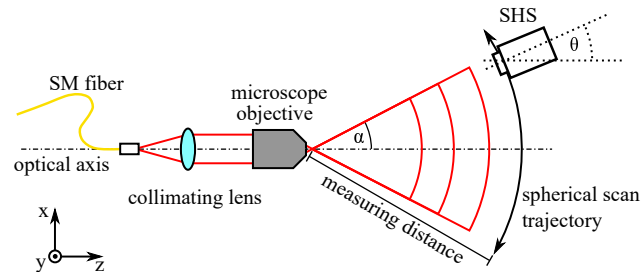


Figure 2. Basic concept of the scanning SHS approach. Increasing the distance far enough to limit the wavefront curvature incident on the sensor while tangentially aligning it to compensate for the incidence tilt. Reconstruction of the global wavefront requires positioning information and registration algorithms (adapted from Ref. 17).

3. EXPERIMENTAL SETUP

Layout and components

To experimentally validate the approach discussed in the previous section, an experimental setup is designed. It consists of 3 translational stages (VT-80 from PI Physik Instrumente, Germany) that offer a positioning resolution of 500 nm and bidirectional repeatability of 10 μm . Further, 2 rotational stages are integrated, one is the RM-3 model from Newmark Systems Inc., United States, the other is the RS-40 from PI Physik Instrumente, Germany. They offer continuous rotation and repeatabilities in the μrad -range. The Shack-Hartmann sensor (HR-2 model from Optocraft, Erlangen, Germany) is mounted in a way that the axes of rotation of both rotation stages intersect in the center of its lenslet array (see Figure 3a) for comparison) and the stages are arranged such that the position- and orientation-coordinates are independent of each other. In a static configuration, the SHS offers an aperture of 11.2×7 mm, with 4 505 lenslets and $\pm 10^\circ$ of maximum incidence angle. Figure 3b) shows a photograph of the complete setup in the laboratory, together with the sample under test.

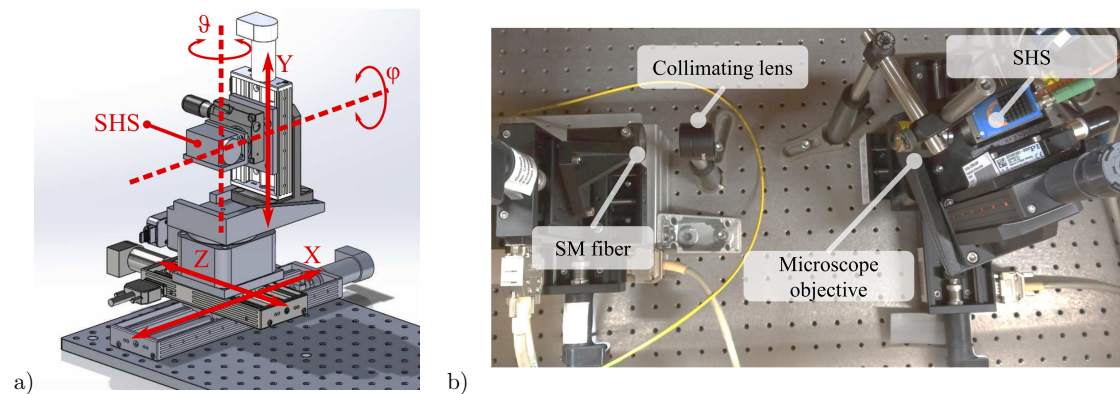


Figure 3. The experimental scanning SHS setup. a) CAD drawing of the motorized setup, consisting of 3 translational and 2 rotational stages. b) Photograph of the experimental setup with a single-mode optical fiber for illumination, a collimating lens, a microscope objective (which is the sample under test) and the scanning SHS.

Measurement strategy

The measurements are conducted by automatically moving the sensor along the wavefront and automatically reorienting it tangentially in each measurement position.¹⁷ The flowchart in Figure 4 illustrates the measurement process and Figure 5 illustrates the feedback loop. Both the strategy and the feedback loop are extended from circular trajectories and 1-dimensional reorientation to spherical sampling trajectories and 2-dimensional reorientation.

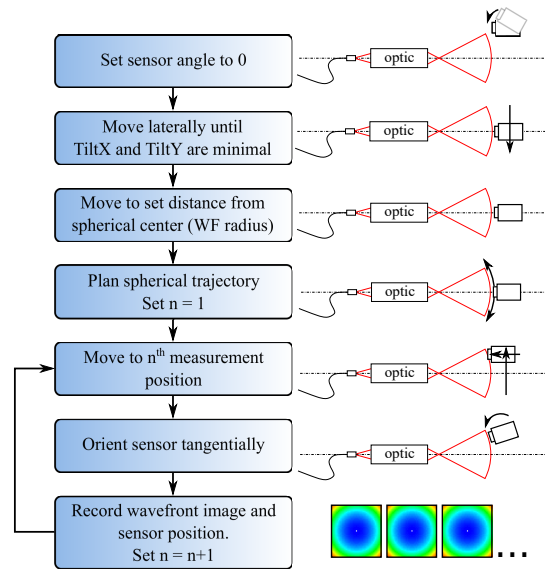


Figure 4. Automated measurement strategy realized on the designed experimental setup. After an initial, manual coarse alignment, the SHS is automatically fine-aligned before stepping through the required measurement positions for acquiring the global wavefront. In each measurement position, the sensor is automatically aligned (see Figure 5 for details). (Figure adapted from Ref. 17.)

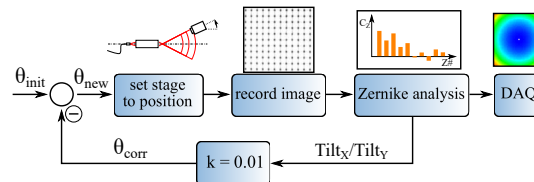


Figure 5. In each of the measurement positions, the SHS needs to be tangentially aligned in order to utilize its whole aperture. The tangential alignment is automated by rotating the sensor until the detected tip- and tilt- Zernike coefficients are close to zero (adapted from Ref. 17).

Registration algorithm

Due to positioning errors accumulated in the positioning system, the recorded subapertures need to be registered numerically to represent the global wavefront. This registration algorithm needs to consider not only translational and rotational errors, but also mismatches in the wavefront propagation.¹⁹ As the recently developed iterative fast parallel registration algorithm (IFPR) is the best-suited for registration of highly divergent wavefronts, it is utilized for the presented experiments.²⁰ The algorithm operates by placing all of the measured subapertures in a common coordinate system. Due to imperfections of the positioning system and small, unknown misalignments

and offsets in the range of single micrometers and mrad, the subsegments show considerable differences in the overlap regions. Then, a global mismatch metric is minimized by varying the 6 rigid-body degrees-of-freedom and one propagation degree-of-freedom of all subapertures simultaneously. After a few (3-4) iterations, this results in a stitched global wavefront with a remaining overlap mismatch of only tens on nm, which is in the same magnitude range as the uncertainty of single SHS measurements.²⁰

4. EXPERIMENTAL RESULTS

To validate the capabilities of the scanning SHS setup, the wavefront generated by a microscope objective is measured. As depicted in Figure 3b), the microscope is illuminated with a collimated beam of light from a 635 nm laser diode (CPS635R, Thorlabs, United States) transmitted via a single-mode fiber (for spatial beam filtering) and collimated by an achromatic lens (AC254-050-A-ML, Thorlabs, United States). The microscope objective is an Olympus DPlan 40x with a numerical aperture of 0.65, corrected for 0.17 mm cover glass. A set of measurement positions is chosen such that the spherical wavefront is sampled by 67 subapertures with 7 mm diameter in a distance of 25 mm from the focus of the microscope objective with an areal overlap of 35% between adjacent subapertures. The measurement is then conducted in an automated fashion as described in Section 3 and registered with the developed iterative fast parallel registration (IFPR) algorithm.²⁰

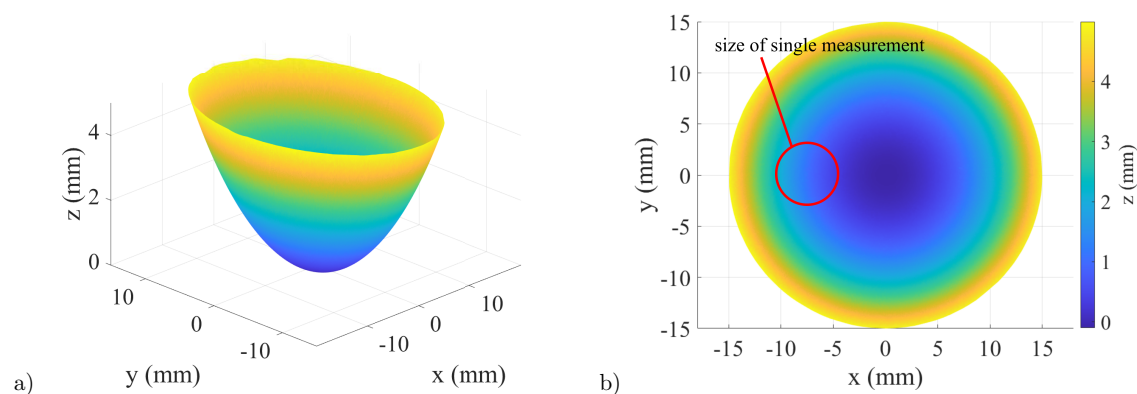


Figure 6. Measurement results on a microscope objective with $NA = 0.65$. a) 3D representation of the global wavefront, comprising 67 subaperture measurements. b) Top-down view of the wavefront, the size of a single subaperture (diameter 6.4 mm) is indicated for comparison.

Figure 6 shows the results of the measurement. In Figure 6a), a 3D representation of the global wavefront is given, while Figure 6b) present a top-down view of the wavefront. Effectively, this represents the wavefront as it would be detected by a SHS with a 30 mm aperture, a maximum incidence angle of $\arcsin(0.65) = \pm 40^\circ$ and a lenslet number of about 41 000. This exceeds the parameters of the utilized SHS by far, which are given as $\pm 10^\circ$ of incidence angle, 4 505 lenslets and an 11.2×7 mm aperture. The red circle in Figure 6b) indicates the size of a single recorded subaperture (diameter 7 mm) for comparison.

To evaluate the quality of the microscope objective under test, the ideal wavefront shape (for perfect focusing) needs to be removed, which is a sphere. Figure 7 displays the remaining wavefront error after a best-fitted sphere is subtracted from the measured wavefront. This analytic step reveals some localized wavefront errors (spikes in the 3D representation, red and blue spots in the top-down view) attributable to dust or scratches within the microscope objective. The root-mean-square (rms) value of this remaining wavefront error is calculated to be 0.62λ .

To further analyze the remaining wavefront aberrations, the outliers (spikes) are removed and a Zernike decomposition of this sphere-corrected wavefront is performed. The outliers are removed by neglecting all points whose absolute value surpasses a threshold of 0.001 mm. Figure 8 shows the resulting Zernike coefficients after fitting

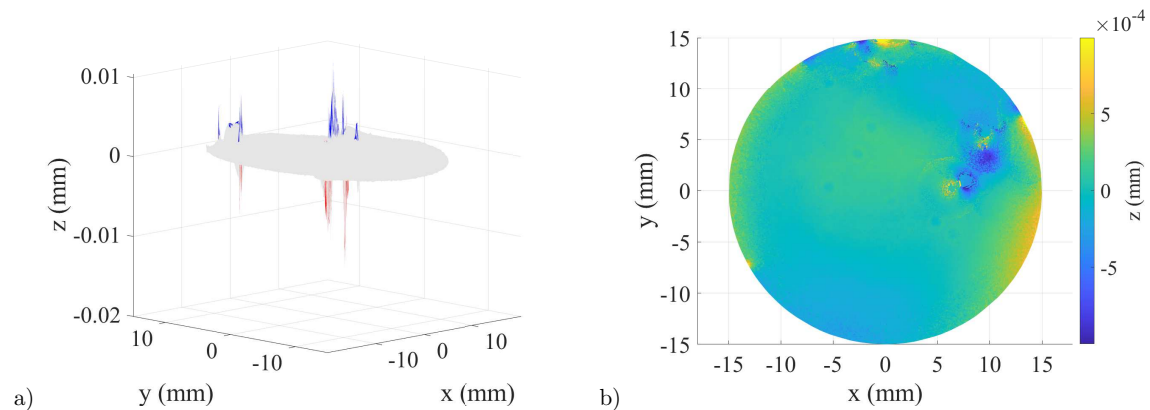


Figure 7. Measurement results on a microscope objective with $NA = 0.65$ after subtraction of a spherical (reference) wavefront. Errors attributable to dust or small scratches can be identified as pronounced peaks. a) 3D representation of the remaining wavefront error. b) Top-down view of the remaining wavefront error after removal of outliers. The rms error value amounts to 0.2767λ or $0.176 \mu\text{m}$.

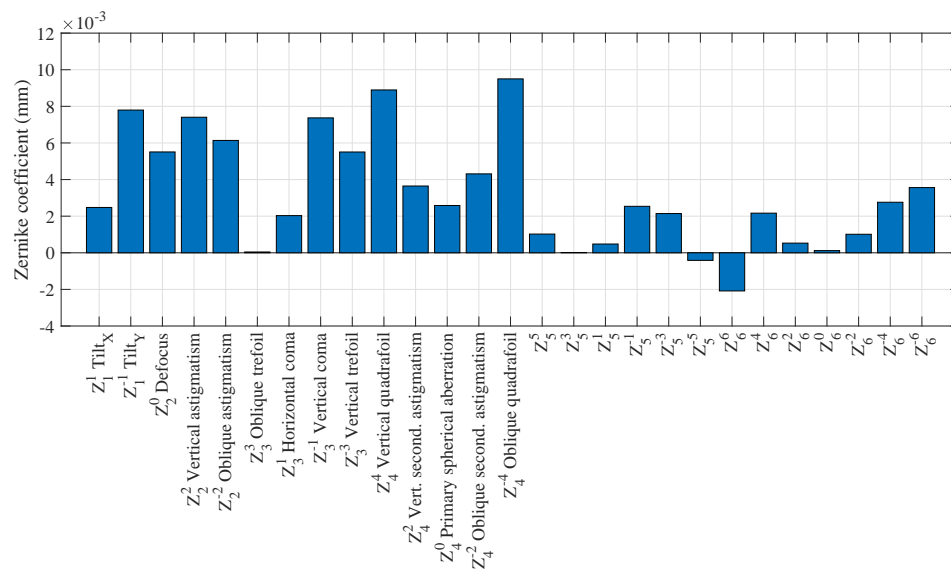


Figure 8. Results of a Zernike decomposition of the measured wavefront. The first 27 Zernike polynomials were fitted to the wavefront after subtraction of the reference sphere and removal of outliers as visible in Figure 7.

the first 27 Zernike polynomials to the wavefront aberrations as shown in Figure 7. The remaining wavefront error is calculated to be $0.176 \mu\text{m}$ or 0.28λ .

In summary, it is successfully shown that the 5-degree-of-freedom scanning SHS setup with automatic alignment and positioning can overcome the dynamic range limitations of a static SHS and - in combination with suitable registration algorithms - directly record a highly divergent optical wavefront generated by a microscope objective with a numerical aperture of 0.65.

5. CONCLUSION AND OUTLOOK

This paper demonstrates the capability of a scanning Shack-Hartmann sensor setup to directly and automatically measure optical wavefronts exceeding the aperture size and the dynamic range of conventional SHS. By combining a 5 degree-of-freedom positioning system with a tailored measurement strategy and a customized registration algorithm, a highly divergent wavefront generated by a microscope objective with a numerical aperture of 0.65 is directly measured, without any collimating optics. After numerically removing outliers and subtracting the reference wavefront, a wavefront error of $0.176 \mu\text{m}$ or 0.28λ remains. This approach is expected to be also well-suited for the quality control of freeform optical parts, provided they can be evenly illuminated and their designed shape is known well enough to plan a measurement trajectory. Future work will focus on developing adaptive trajectory-planning to alleviate the need for a-priori knowledge of the wavefront shape and advanced post-processing steps to make the measured data directly comparable to other metrology approaches, such as interferometric techniques for freeforms.

ACKNOWLEDGMENTS

The financial support by the Christian Doppler Research Association, the Austrian Federal Ministry for Digital and Economic Affairs, and the National Foundation for Research, Technology and Development is gratefully acknowledged.

REFERENCES

- [1] Nikolov, D. K., Bauer, A., Cheng, F., Kato, H., Vamivakas, A. N., and Rolland, J. P., "Metaform optics: Bridging nanophotonics and freeform optics," *Science Advances* **7**(18), eabe5112 (2021).
- [2] Rolland, J. P., Davies, M. A., Suleski, T. J., Evans, C., Bauer, A., Lambropoulos, J. C., and Falaggis, K., "Freeform optics for imaging," *Optica* **8**(2), 161–176 (2021).
- [3] Lamontagne, F., Fuchs, U., Trabert, M., and Möhl, A., "Aspheric lens mounting," *International Optical Design Conference 2017* **57**(10), 7 (2017).
- [4] Fang, F., Zhang, X., Weckenmann, A., Zhang, G., and Evans, C., "Manufacturing and measurement of freeform optics," *CIRP Annals* **62**(2), 823–846 (2013).
- [5] Chen, S., Xue, S., Zhai, D., and Tie, G., "Measurement of freeform optical surfaces: Trade-off between accuracy and dynamic range," *Laser & Photonics Reviews* **14**(5), 1900365 (2020).
- [6] Kim, B. C., Saiag, T., Wang, Q., Soons, J., Polvani, R. S., and Griesmann, U., "The geometry measuring machine (gemm) project at nist," in [*Free-Form Optics: Design, Fabrication, Metrology, Assembly, ASPE 2004 Winter Topical Meeting*], 108–111 (2004).
- [7] Burge, J. H., "Applications of computer-generated holograms for interferometric measurement of large aspheric optics," in [*International Conference on Optical Fabrication and Testing*], **2576**, 258–269, International Society for Optics and Photonics (1995).
- [8] Dai, G., Bütetisch, S., Pohlenz, F., and Danzebrink, H.-U., "A high precision micro/nano cmm using piezoresistive tactile probes," *Measurement Science and Technology* **20**(8), 084001 (2009).
- [9] Henselmans, R., Cacace, L., Kramer, G., Rosielle, P., and Steinbuch, M., "The nanomefos non-contact measurement machine for freeform optics," *Precision Engineering* **35**(4), 607 – 624 (2011).
- [10] Platt, B. C. and Shack, R., "History and Principles of Shack-Hartmann Wavefront Sensing," *Journal of Refractive Surgery* **17**(5), S573–S577 (2001).
- [11] Thier, M., Paris, R., Thurner, T., and Schitter, G., "Low-latency shack-hartmann wavefront sensor based on an industrial smart camera," *IEEE Transactions on Instrumentation and Measurement* **62**(5), 1241–1249 (2013).
- [12] Burada, D. R., Pant, K. K., Bichra, M., Khan, G. S., Sinzinger, S., and Shakher, C., "Experimental investigations on characterization of freeform wavefront using shack-hartmann sensor," *Optical Engineering* **56**(8), 084107 (2017).
- [13] Pant, K. K., Burada, D. R., Bichra, M., Singh, M. P., Ghosh, A., Khan, G. S., Sinzinger, S., and Shakher, C., "Subaperture stitching for measurement of freeform wavefront," *Applied Optics* **54**(34), 10022 (2015).

- [14] Rocktäschel, M. and Tiziani, H. J., “Limitations of the Shack-Hartmann sensor for testing optical aspherics,” *Optics and Laser Technology* **34**(8), 631–637 (2002).
- [15] Fuerst, M. E. and Schitter, G., “Scanning wavefront sensor for measurement of highly divergent wavefronts,” *IFAC-PapersOnLine* **52**(15), 25–30 (2019).
- [16] Fuerst, M. E., Berlakovich, N., Csencsics, E., and Schitter, G., “Self-aligning scanning shack-hartmann sensor for automatic wavefront measurements of high-na optics,” in [2020 *IEEE International Instrumentation and Measurement Technology Conference (I2MTC)*], 1–6, IEEE (2020).
- [17] Fuerst, M. E., Csencsics, E., Berlakovich, N., and Schitter, G., “Automated measurement of highly divergent optical wavefronts with a scanning shack–hartmann sensor,” *IEEE Transactions on Instrumentation and Measurement* **70**, 1–9 (2020).
- [18] Mauch, S. and Reger, J., “Real-time spot detection and ordering for a shack–hartmann wavefront sensor with a low-cost fpga,” *IEEE Transactions on Instrumentation and Measurement* **63**(10), 2379–2386 (2014).
- [19] Berlakovich, N., Csencsics, E., Fuerst, M., and Schitter, G., “Fast, precise, and shape-flexible registration of wavefronts,” *Applied Optics* **60**(23), 6781–6790 (2021).
- [20] Berlakovich, N., Csencsics, E., Fuerst, M., and Schitter, G., “Iterative parallel registration of strongly misaligned wavefront segments,” *Optics Express* **29**(21), 33281–33296 (2021).